JOURNAL OF MAGNETIC RESONANCE **129,** 219–221 (1997)
ARTICLE NO. MN971279

Effect of Sweep Direction on Sidebands in Adiabatic Decoupling

Ēriks Kupče

Varian NMR Instruments, 28 Manor Road, Walton-on-Thames, Surrey, KT12 2QF, England

E-mail: eriks.kupce@nmr.varian.com

Received April 16, 1997; revised September 5, 1997

The appearance of sidebands in adiabatic decoupling can be substantially reduced simply by matching the sweep rate and direction of adiabatic pulses with the evolution of different *J* couplings. Alternatively, a matched adiabatic defocusing pulse is applied just before the decoupling is turned on, providing an efficient means for complete suppression of sidebands.

Adiabatic decoupling has several important advantages over the traditional composite pulse decoupling methods—high tolerance to the RF field inhomogeneity and miscalibration, more efficient use of the RF power, and extremely wide effective bandwidth (*1*). Several decoupling schemes based on hyperbolic secant (sech) (*2, 3*), chirp (*4, 5*), and WURST (*6, 7*) adiabatic passages have been introduced earlier. Unfortunately, all these methods suffer from relatively intense decoupling sidebands (*3, 7*), especially at very high magnetic fields where increasingly wide spectral regions need to be covered (see Fig. 1). As shown in the present work, in many practical situations the appearance of decoupling sidebands can be substantially reduced simply by matching the sweep rate and direction with the evolution of *J* couplings. A simple adiabatic defocusing pulse applied just before the decoupling is turned on provides an efficient means for complete suppression of decoupling sidebands.

Most of the decoupling test experiments employ a simple model compound, for example, MeJ, and therefore are based on an assumption that the coupling constants have similar magnitudes over the entire decoupling bandwidth. However, in many practical applications, for instance, in ^{13}C-decoupled experiments, this is not the case. Furthermore, in many coherence transfer experiments the *J*-refocusing period which occurs just before the decoupling is turned on leaves a certain amount of residual antiphase magnetization due to the fact that larger *J* couplings in the aromatic region refocus at an earlier stage than smaller couplings in the aliphatic domain. The amount of this antiphase magnetization, which also contributes to the decoupling sidebands (*8, 9*), depends on the time difference (ΔT) between the refocusing periods of the largest and smallest couplings in the given spin system,

$$\Delta T = 0.5/J_{\max} - 0.5/J_{\min}, \qquad [1]$$

where $J_{\max}$ and $J_{\min}$ are the maximum and minimum couplings to be decoupled.

The subharmonic sidebands which appear with increasing intensity toward the edges of the decoupling bandwidth (see Fig. 1c) are caused by the distorted symmetry of the *J*-refocusing process for spins inverted at the beginning and end of the frequency sweep (*7*) during the adiabatic decoupling. This asymmetry can be readily compensated for by adjusting the sweep rate and direction such that they match the evolution of spin couplings.

As an example, three traces representing the most intense peaks in the middle and on both edges of a WURST-20-decoupled ^{13}C HSQC spectrum of brucine are shown in Fig. 2. A relatively long adiabatic sweep of 2 ms was used in order to enhance the appearance of the sidebands. In the upper part of Fig. 2 the sweep direction was from high frequency (aromatics) to low frequency (aliphatics) and the sweep rate *k* was set according to

$$k = \Delta\nu/\Delta T, \qquad [2]$$

where $\Delta\nu$ is the frequency difference between the signals corresponding to $J_{\max}$ and $J_{\min}$ and ΔT is given by Eq. [1]. The subharmonic sidebands have essentially been eliminated. In the lower part of Fig. 2 the same decoupling scheme was used, except that the sweep direction is opposite—from low to high frequencies. The subharmonic sidebands appear with full strength and are higher for peaks with larger couplings.

Obviously, such an approach can be successfully employed only if there is a roughly linear correlation between the spin–spin coupling constants and the chemical shifts of X nuclei (*10, 11*). However, there are many situations where such a relationship does not exist, for example, in N–H correlated spectra or in experiments which do not employ coherence transfer from nuclei to be decoupled, for instance, H–H correlated experiments (NOESY, TOCSY, etc.) with isotopically enriched proteins. In this case the required asymmetry can be created artificially using an appropriate adiabatic defocusing (ADF) pulse.

1090-7807/97 $25.00

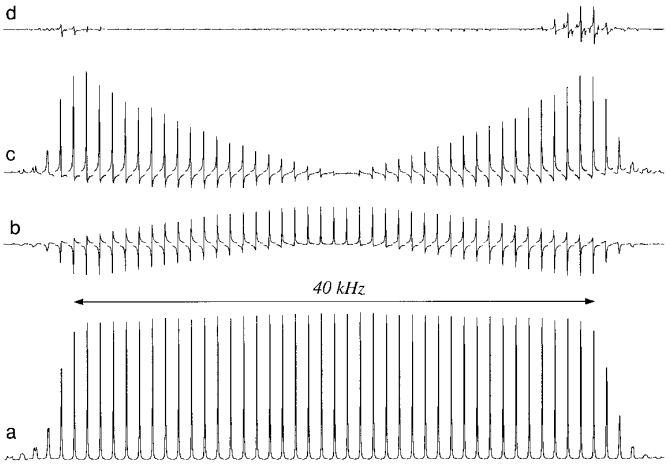

FIG. 1. Decoupling sidebands generated using a WURST-40 waveform. (a) The decoupling profile, (b) the principal sidebands appearing at $1/T_d$, (c) the subharmonic sidebands appearing at $1/2T_d$, and (d) residual sidebands after the subharmonic component was eliminated using the SEAD scheme shown in Fig. 3. The vertical scale in traces (b)–(d) is increased by a factor of 10. A relatively long pulse of $T_d = 2$ ms was used to enhance the outer decoupling sidebands. A high adiabaticity factor $Q = 3.0$ giving $B_1(\max)$ of 3.0 kHz ($B_1(\mathrm{RMS}) = 2.8$ kHz) was employed in order to suppress the inner sidebands.

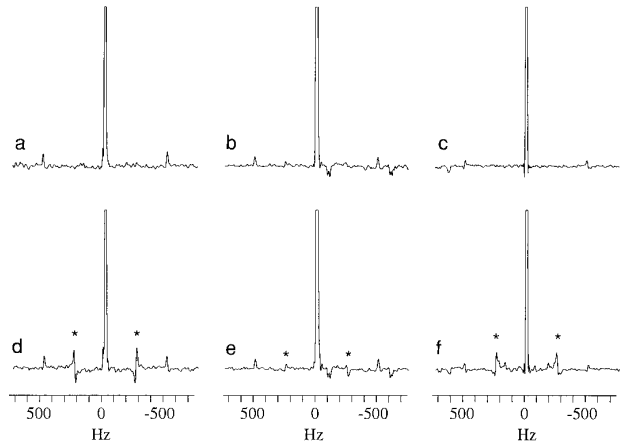

FIG. 2. Selected traces from 2D ^{13}C HSQC spectra of brucine recorded on a Varian Unity Plus spectrometer operating at 500 MHz proton frequency. Signals corresponding to (a) aromatic CH ($\delta_C = 102.2$ ppm, $J_{CH} = 159$ Hz), (b) OCH (60.6 ppm, 143 Hz), and (c) TMS (0.0 ppm, 118 Hz) added as a reference are shown. All traces are truncated at the 25% level. The upper traces (a) to (c) are from an experiment using a matched WURST-20 decoupling waveform sweeping from higher to lower frequencies at a rate of 12.5 MHz/s, $T_d = 2$ ms, $B_1(\max) = 3.0$ kHz, $B_1(\mathrm{RMS}) = 2.8$ kHz. The subharmonic sidebands are virtually absent in this experiment. The lower traces (d) to (f) are from an identical experiment, except the sweep direction of decoupling waveform was opposite. As expected, the subharmonic sidebands appear with increasing intensity toward the edges of the decoupling bandwidth (traces (e) and (f)). Refocusing delays of 1.47 ms were used.

A simple pulse sequence (see Fig. 3) is used to demonstrate this approach. Assuming that (1) spin flip is instantaneous, (2) spin inversion is complete, and (3) phase evolution is linear during the experiment,[1] the experiment can be analyzed using the phase diagram (*10*) shown in Fig. 3.

The most efficient decoupling is achieved when the extent of J defocusing during decoupling is the same over the entire decoupling bandwidth. Because of the asymmetry of spin inversion during the adiabatic sweep, the J defocusing is at a minimum in the midpoint of the decoupling pulse (*7*). Ideally we would require the same extent of J defocusing also at any other point of the decoupling pulse. In the scheme shown in Fig. 3 this can be achieved if the sweep direction of the ADF pulse (T_p) is reversed with respect to that of the decoupling waveform (T_d). By requiring the minimum J defocusing of $\pm JT_d/2$ at the beginning

$$\Delta - T_p - \Delta + T_d = T_d/2 \qquad [3]$$

and end

$$\Delta + T_p - \Delta - T_d = -T_d/2 \qquad [4]$$

of the adiabatic decoupling pulse we arrive at the condition $T_p = T_d/2$. It can easily be demonstrated that the minimum J defocusing of $\pm JT_d/2$ is now achieved at any other point of the decoupling pulse. Note that the Δ delays have no effect on the extent of J defocusing. The effect of the ADF pulse (with Δ set to zero) on the subharmonic sidebands is demonstrated experimentally in Fig. 1d.

The first and higher harmonics (Fig. 1b) can readily be

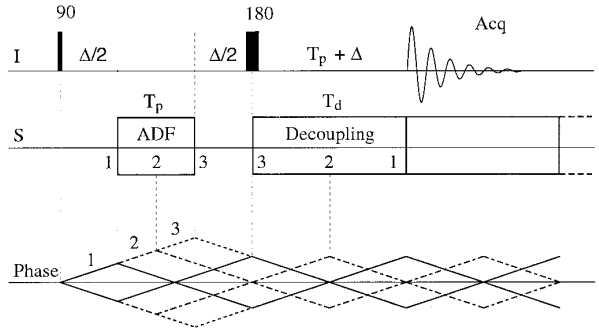

FIG. 3. Sideband elimination by adiabatic defocusing (SEAD) and the corresponding phase evolution diagram. The spins flipped at the beginning, middle, and end of the adiabatic sweep are denoted by 1, 2, and 3. Note that the sweep direction is opposite for the adiabatic defocusing (ADF) pulse of length T_p and the decoupling pulse of length $T_d = 2T_p$. The frequency sweep range is equal for both pulses. The ADF pulse ensures that the phase excursions are at a minimum ($\pm JT_d/2$) and are equal for all spins within the decoupled bandwidth during the adiabatic decoupling.

[1] In fact the phase evolution is not strictly linear because of the presence of the decoupling field. However, this appears to have a little effect under the given experimental conditions.

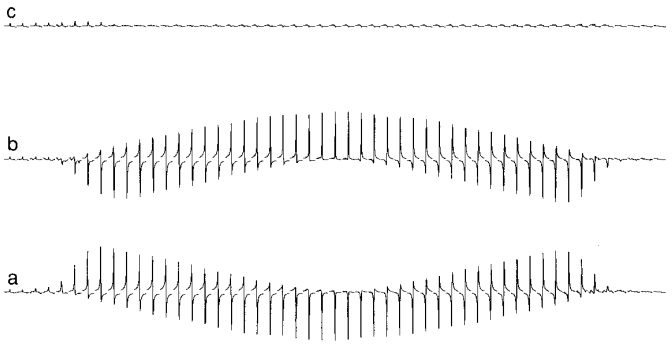

FIG. 4. Effect of time (Δ) incrementation in the SEAD experiment (Fig. 3) on the phase of the principal sidebands in WURST-40 decoupling. (a) $\Delta = 0.0$, (b) $\Delta = 0.5T_d$, and (c) sum of (a) and (b). A WURST-20 inversion pulse of length $T_p = 1.0$ ms and adiabaticity $Q = 4$ was used for adiabatic defocusing. The other parameters are the same as in the legend to Fig. 1.

eliminated by shifting the beginning of acquisition with respect to the decoupling waveform, provided that magnetization is in the XY plane when the decoupling is switched on (*9*). This can readily be achieved by incrementing the delay Δ in steps of T_d/N, where N is the total number of increments. As shown in Fig. 4 the first (principal) harmonic can be eliminated in just two steps, with Δ set to zero and $T_d/2$, whereas a four-step cycle ($\Delta = 0$, $T_d/4$, $T_d/2$, and $3T_d/4$) is necessary to eliminate the second harmonic. Since the intensity of the outer sidebands is rapidly decreasing with n, in most applications the two-step cycle will suffice. We call this experiment SEAD (sideband elimination by adiabatic defocusing).

The SEAD technique is more efficient than the sideband distribution strategy suggested earlier (*2, 12, 13*), is simpler to implement than the bilevel decoupling technique (ECO-WURST) (*9*), and does not require high peak amplitude used to suppress the subharmonic sidebands in ECO-WURST (*9*) and echo-WURST (*10*) schemes.

The implantation of SEAD into the refocusing period of coherence transfer experiments is straightforward—the conventional inversion X pulse is replaced by the ADF pulse and the Δ delay is incremented as described above. SEAD can also be combined with the natural evolution of J couplings in spins systems where there is a linear correlation between J couplings and chemical shifts. Alternatively, a pre-SEAD 90° purge (X) pulse may be necessary to remove any antiphase components (*9*). A more detailed description of the approach used here to describe experiments involving adiabatic pulses was given earlier (*10*).

To conclude, it has been demonstrated that the direction of the frequency sweep in adiabatic decoupling schemes has a considerable effect on the intensity of decoupling sidebands. Simple schemes have been suggested for efficient elimination of these sidebands.

REFERENCES

1. Ē. Kupče, R. Freeman, G. Wider, and K. Wüthrich, *J. Magn. Reson. A* **120,** 264 (1996).
2. Z. Starčuk, Jr., K. Bartušek, and Z. Starčuk, *J. Magn. Reson. A* **107,** 24 (1994).
3. T. E. Skinner and M. R. Bendall, *J. Magn. Reson. A* **123,** 111 (1996).
4. V. J. Basus, P. D. Ellis, H. D. W. Hill, and J. S. Waugh, *J. Magn. Reson.* **35,** 19 (1979).
5. R. Fu and G. Bodenhausen, *Chem. Phys. Lett.* **245,** 415 (1995).
6. Ē. Kupče and R. Freeman, *J. Magn. Reson. A* **115,** 273 (1995).
7. Ē. Kupče and R. Freeman, *J. Magn. Reson. A* **117,** 246 (1995).
8. M. H. Levitt, G. Bodenhausen, and R. R. Ernst, *J. Magn. Reson.* **53,** 443 (1983).
9. Ē. Kupče, R. Freeman, G. Wider, and K. Wuthrich, *J. Magn. Reson. A* **122,** 81 (1996).
10. Ē. Kupče and R. Freeman, *J. Magn. Reson.* **127,** 36 (1997).
11. C. Zwahlen, P. Legault, S. J. F. Vincent, J. Greenblatt, R. Konrat, and L. E. Kay, *J. Am. Chem. Soc.* **119,** 6711 (1997).
12. T.-L. Hwang, M. Garwood, A. Tannus, and P. C. M. van Zijl, *J. Magn. Reson. A* **121,** 221 (1996).
13. T. E. Skinner and M. R. Bendall, *J. Magn. Reson. A* **124,** 474 (1997).